#296: Coupling ventilated photovoltaic window with air-conditioning system: electrical, thermal, and daylight performance for different window-to-wall ratios

Yayun TANG[1], Jie JI[2], Chengyan ZHANG[3], Chuyao WANG[4]

[1] Department of Thermal Science and Energy Engineering, University of Science and Technology of China, Hefei, Anhui, China. tangyayun@mail.ustc.edu.cn
[2] Department of Thermal Science and Energy Engineering, University of Science and Technology of China, Hefei, Anhui, China. jijie@ustc.edu.cn
[3] Department of Thermal Science and Energy Engineering, University of Science and Technology of China, Hefei, Anhui, China. zcy19013@mail.ustc.edu.cn, China.
[4] Department of Building Environment and Energy Engineering, The Hong Kong Polytechnic University, Hong Kong, China. chuyao.wang@polyu.edu.hk

Abstract: Solar energy, owing to its emission-free properties and environmental sustainability, has been extensively explored for integration into buildings. Building-integrated photovoltaic (BIPV) technology contributes to energy conservation and emissions reduction by combining electricity generation with architectural design. However, conventional solar buildings face challenges related to single functionality, suboptimal photoelectric conversion, and a significant increase in space cooling load. In response, a semi- transparent BIPV window system combined with an air-conditioning system is proposed as a promising solution to improve comfort levels and reduce energy consumption. This study aims to provide valuable insights into optimizing system designs for achieving more energy-efficient buildings. The focus is on evaluating the energy and daylight performance of this combined system for various window-to-wall ratios (WWR). Electrical and thermal performance is simulated and assessed through solutions of the energy balance equations for each component of the system in the Matlab environment. Daylighting simulations are conducted using Design Builder software to analyze the distribution of natural light in indoor spaces and thus artificial lighting demand. Furthermore, the influence ofWWR on the energy benefits and consumption of a typical office integrated with this system is investigated for three typical cities inChina with hot-humid weather conditions. Results show that with a relatively large WWR (WWR ≥ 60%), the application of the system in the building offers better overall energy performance.

Keywords: PV Window, Power Generation, Air-Conditioning System, Lighting Energy, Building Energy Consumption

1. INTRODUCTION

As the world transitions towards sustainable energy technologies, integrating renewable energy sources into buildings becomes increasingly important. Semi-transparent photovoltaic windows (STPV-W) represent a promising technology that replaces conventional glass with STPV modules, providing both daylighting and clean electricity generation.

STPV has received extensive attention from scholars due to its potential benefits. Wang et al. (Wang et al., 2016) investigated the optical, electrical, and thermal performance of a ventilated STPV-W using a mathematical model developed with EnergyPlus software. Their findings revealed that replacing single-layer transparent glass with STPV insulating glass could save up to 25.3% ofenergy. Yadav et al. (Yadav and Hachem-Vermette, 2024) examined a STPV system composed of an air layer, glass panels, and curtains. Their study found that the system generated 361 Wh/m^2 of electricity daily, and it effectively reduced heating demand in cold weather while decreasing cooling energy consumption in hot climates. Tan et al. (Tan et al., 2023) developed a numerical model for vacuum PV glass units using Python, validating the model's accuracy with experimental test data. The units demonstrated excellent thermal insulation performance, with a U-value of less than 1.0 W/m²·K. Additionally, a vacuum glass component with a 90% PV coverage ratio had an annual output of 24.77 kWh/m^2. PV coverage ratios exceeding 50% maintained good visual comfortfor occupants, with negligible discomfort glare. Qiu et al. (Qiu and Yang, 2022) combined STPV cells with vacuum glass, showing that the typical winter day heat flux density could reach approximately 250 W/m^2.

Despite these advancements, research on STPV modules has primarily focused on the thermal and electrical performance of the PV cells themselves. There has been less research that comprehensively considers the power generation performance of STPV-Wsystems and their impact on indoor air conditioning and daylighting, particularly with regard to the coupled operation of STPV-W and air conditioning systems under different window-to-wall ratios (WWR).

This study aims to address this gap by investigating the potential of coupling an air-conditioning system with a ventilated STPV-W in hot-humid weather conditions. The focus is on evaluating the electrical, thermal, and daylighting performance of this combined system for various WWRs.

2. METHODOLOGY

This section presents the system configuration and simulation methodology.

2.1 Structure of the STPV-W

Figure 1 illustrates a cross-section of a ventilated double-glazing STPV-W. The outdoor-facing PV glazing consists of a laminated PV film layer sandwiched between exterior and interior tempered glass, with a PV coverage ratio of 0.8. The interior side features common clear tempered glass, creating an air channel between it and the PV glazing.

In summer, when the air conditioning system is operational, supply air cooled to the dew-point state by an air handling unit (AHU) is introduced into the air channel of the STPV-W. The STPV-W converts solar irradiation into electrical energy while preheating the supply air at the dew point. An electric heating device then assists in raising the supply air temperature to an acceptable level of 18°C before being delivered into the indoor space. A more detailed description of the system's operating principle can be found in ourpreviously published paper (Tang et al., 2022).

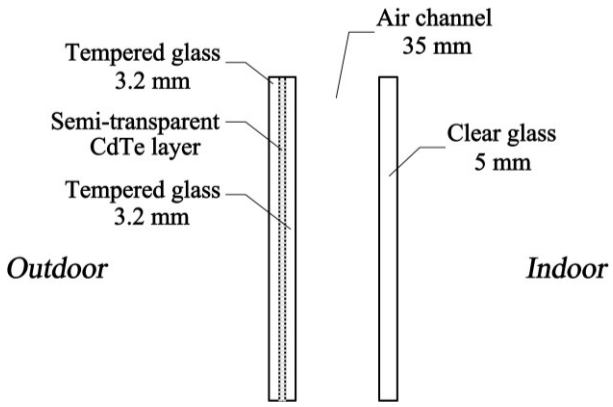

Figure 1: Cross section of the ventilated CdTe thin-film STPV-W

2.2 Performance evaluation model

The power output and electrical efficiency of the solar cells are calculated as

Equation 10: Electrical generation

$$E_{PV} = \int_0^t A_{PV}\tau I\eta_e dt$$

Equation 2: Electrical efficiency

$$\eta_e = \eta_0[1 - Br(T_{PV} - 298.15)]$$

Where:

- E = electrical energy (kWh)
- A_{PV} = area of PV cells (m^2)
- τ = transmittance
- I = incident solar radiation (W/m^2)
- η_0 = PV efficiency under standard testing conditions (Wang et al., 2021)
- Br = temperature coefficient of CdTe PV cells, K^{-1} (Skoplaki and Palyvos, 2009)
- T_{PV} = temperature of PV cells, K
- t = operating time, s

The heat recovered from the PV window is calculated by

Equation 3: Heat recovery

$$Q_{rec,heat} = \int_0^t c_p \dot{m}_{ca}(T_{outlet} - T_{inlet})\, dt$$

Where:

- Q = thermal energy (kWh)
- c_p = specific heat of air (kJ/kg • °C)
- $\dot{m}_{ca}$ = mass flow rate of channel air (kg/s)
- T_{outlet} = temperature of channel outlet air, K
- T_{inlet} = temperature of channel inlet air, K

The fan energy is calculated by

Equation 4: Fan energy

$$E_{fan} = \int_0^t \frac{\Delta P \dot{V}_{sa}}{\eta_{fan}} dt$$

Where:

- ΔP = fan pressure to overcome the flow resistances (Pa)
- V_{sa} = supply air volume flow rate (m^3/s)
- η_{fan} = fan efficiency

The energy benefits of the building incorporating this hybrid system are derived from two sources: the electricity generated by PV cells (E_{PV}) and the heat recovered from STPV-W ($Q_{rec,heat}$). On the other hand, the building's energy consumption encompasses the energy used by the air-conditioning system (E_{AHU}), the supply air fan (E_{fan}), and the artificial lighting (E_{lgt}). The net electricity consumption (NEC) of the building can be calculated using

Equation 5: Quantity of NEC

$$\mathrm{NEC} = E_{AHU} + E_{fan} + E_{lgt} - E_{PV} - Q_{rec,heat}/COP$$

Where:

- COP = coefficient of performance of air-conditioning equipment, which is taken as 3.5(Tang et al., 2022)

2.3 Building characteristics for simulation

An office building was used for the case study, featuring the STPV-W integrated into the south-facing façade and connected to a primary return air-conditioning system. A three-dimensional schematic of the building is shown in Figure 2, with dimensions of 14 m(north-south) × 18 m (east-west) × 4.2 m in height. The building is occupied from 8:00 to 19:00.

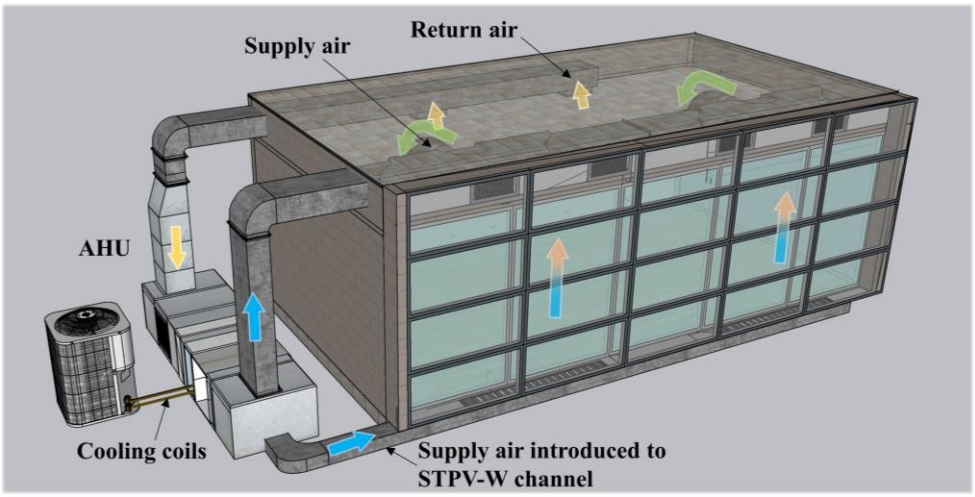

Figure 2: Building prototype integrated with the STPV-W coupled with an air-conditioning system

WWR, the proportion of a building's window area to its total façade area, is a key design factor influencing energy performance (Zhang et al., 2024). High WWR can lead to increased exposure to external weather conditions, affecting indoor environment control. Specifically, a large STPV-W area can make interiors more susceptible to temperature variations on the internal glazing surface. Furthermore, STPV glazing absorbs a portion of incoming solar radiation to generate electricity, while also producing heat and allowing daylight to penetrate. Enlarging the STPV-W area can enhance electricity generation, heat recovery, and natural daylight availability. However, the increased solar heat gain can raise cooling demand in summer by increasing heat gain due to higher solar heat penetration.

Therefore, exploring the optimal WWR is crucial for optimizing the STPV-W system in conjunction with the supply air handling. It involves balancing energy generation and consumption with indoor comfort. This balance ensures maximum energy efficiency by leveraging solar power benefits while minimizing additional energy consumption for room air conditioning and lighting, thus providing valuable design guidance.

In this study, the electrical, thermal, and daylight performance, as well as the net energy consumption (NEC), of the building with WWR of 20%, 40%, 60%, 80%, and 100%, were simulated. The façade design scenarios for different WWRs by changing the STPV- W height, are shown in Figure 3.

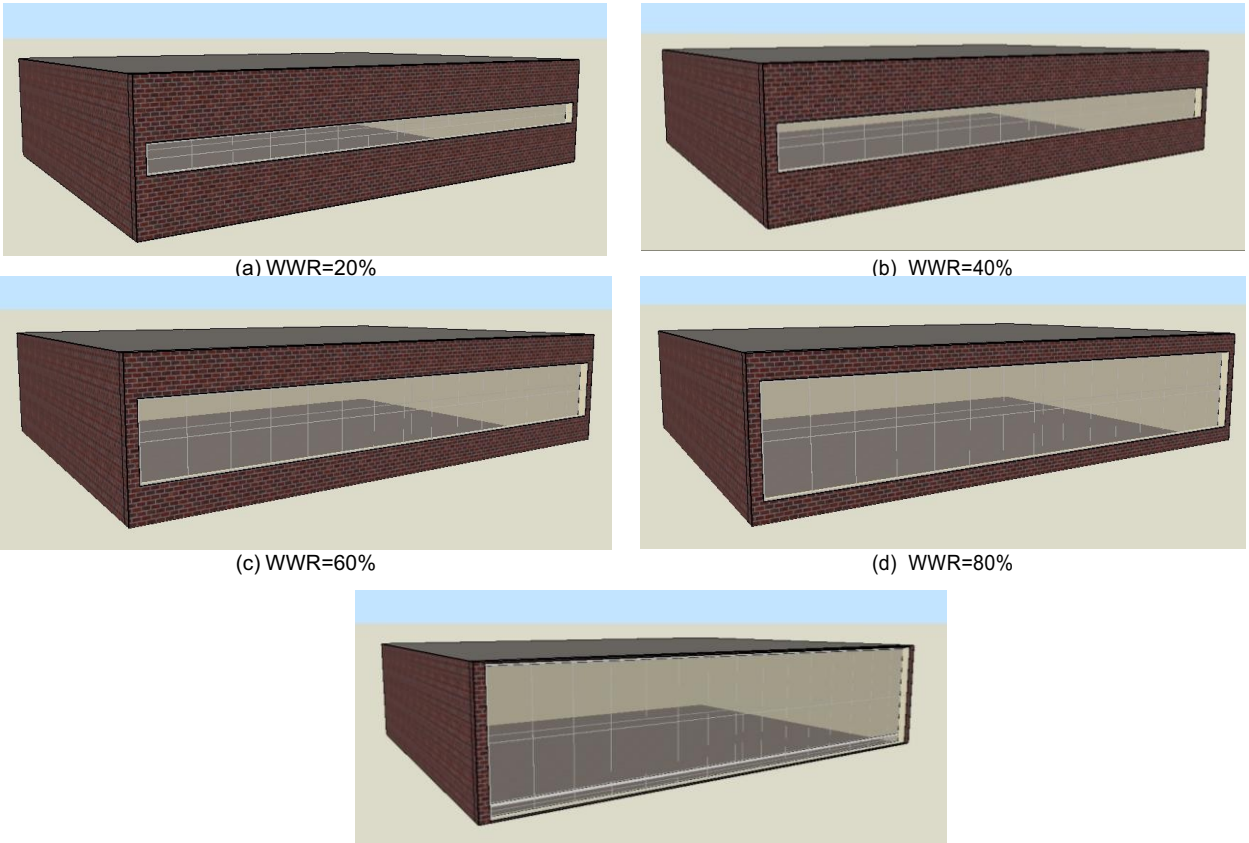

(a) WWR=20%
(b) WWR=40%
(c) WWR=60%
(d) WWR=80%
(e) WWR=100%

Figure 3: Facade design scenarios with varying WWR

2.4 Meteorological conditions for simulation

Locations in China are classified into five climatic zones based on different meteorological characteristics (Zhang et al., 2024). The studied system, designed for hot and humid weather conditions, specifically targets the building's cooling and dehumidification needs in summer. Therefore, the cooling seasons of the cold zone, hot summer and cold winter zone, and hot summer and warm winter zone are selected for the simulation study due to their hot and humid summers. Three cities, each representing one of these climatic regions, are selected as listed in Table 1. Using weather data from June 1 to August 31 of the Typical Meteorological Year (TMY) for these cities, the building performance evaluation was performed in 10 s time steps.

Table 1: Geographic and climatic information of 3 cities for the building simulation

	Climate zone	Latitude	Longitude	Summer avg. temp.	Summer avg. incident solar irradiance
Beijing	Cold	39.9° N	116.3° E	25.47 °C	189.77 kWh/m^2
Hefei	Hot summer and cold winter	31.5° N	117.2° E	26.87 °C	144.93 kWh/m^2
Guangzhou	Hot summer and warm winter	23.1° N	113.3° E	28.02 °C	119.37 kWh/m^2

2.5 Simulation methods and conditions

Electrical and thermal energy simulation

Based on the photoelectric properties of CdTe PV modules and the principles of thermodynamics, we have developed an unsteadycoupled model of the optical-electrical-thermal behavior of the double-glazing window system under forced convection. The output power of the PV module depends on the solar radiation intensity, the PV cell area, and its temperature.

Using the heat balance method, the temperature distribution for each envelope was derived, and the thermal processes affecting the indoor air were analyzed. Initially, the time- and space-dependent energy conservation equations were listed, and the initial and boundary conditions based on weather conditions were mathematically described. The grid nodes for the region defined by these equations were then divided. By discretizing the partial differential equations describing the flow and heat transfer processes using the finite volume method, they were transformed into a set of algebraic equations at each node. These equations were solved through iterative computation using Matlab programming.

In this simulation, the internal equipment and lighting loads are 20 W/m^2 and 11 W/m^2, respectively, and the indoor occupant density is 2.5 m^2/person. The indoor design set point is a temperature of 26 °C and a relative humidity of 60% in summer (Yount, 2017).

Daylight simulation

The annual daylighting performance of the building was modeled and simulated using DesignBuilder software. First, a three-dimensional geometric model of the building was created in DesignBuilder. Then, the optical properties—such as reflectance, transmittance, and absorptance—of each surface in the building model were defined. Subsequently, the sky model, geographic location, simulation time, and weather conditions were configured. The ray-tracing method was employed to analyze the travel of light through the components of each layer of the STPV-W and to model the distribution of natural light within the building's interior (Tang et al., 2022). The working plane was set at a height of 0.75 m above ground, with a target illuminance of 300 lux.

3. RESULT AND DISCUSSION

Figure 4 presents the simulation results for the impact of different WWRs on the performance parameters of the case buildings throughout the summer. Figure 5 illustrates the variations in energy benefits and consumption, and NEC, as the WWR increases.

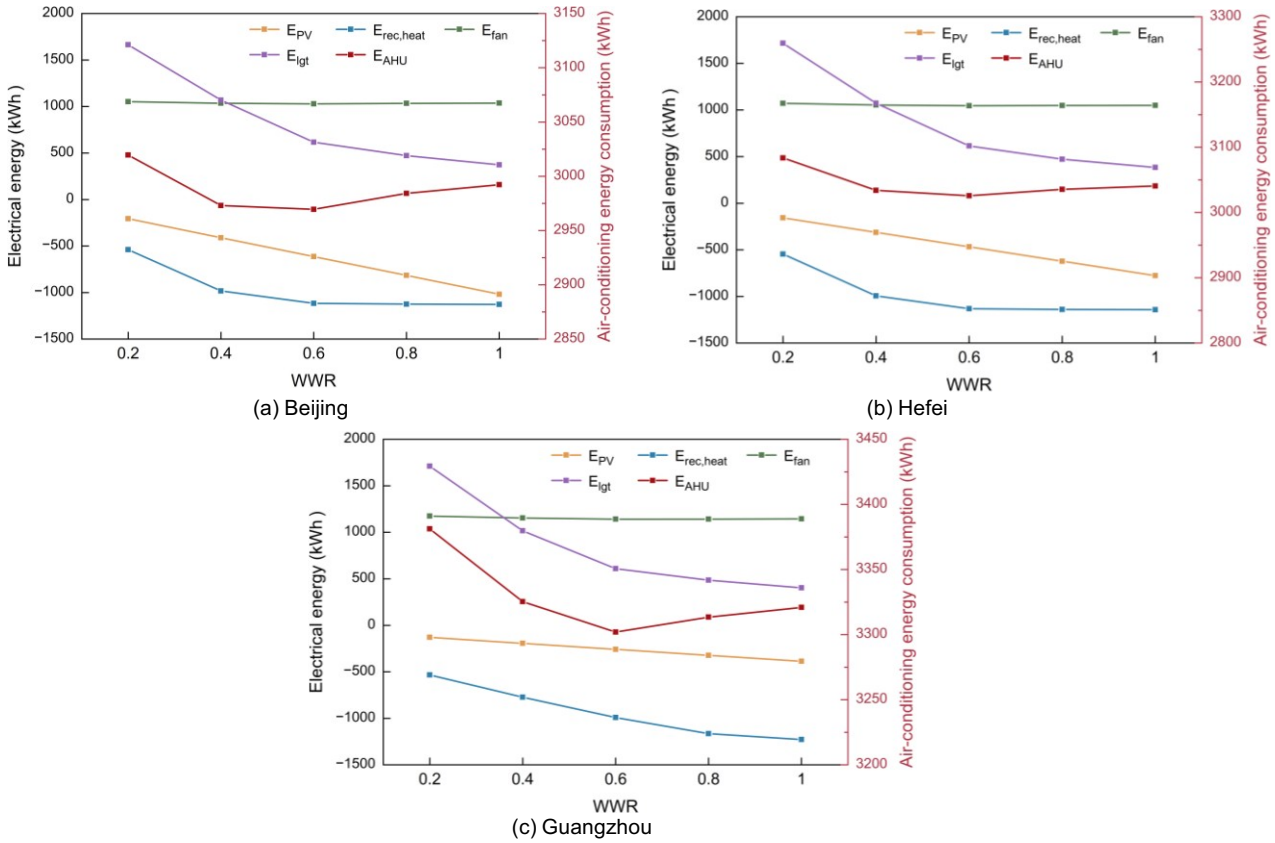

Figure 4: Variations in power generation, heat recovery, air-conditioning energy consumption, fan energy, and lighting demand for different WWRsthroughout the summer.

3.1 Impact of WWR on electricity generation

The amount of solar radiation received by the CdTe thin-film cells is a crucial factor influencing photovoltaic (PV) output. As the WWR increases, the PV glass area expands, allowing more solar irradiation to be incident on the PV glass surface, which is then converted into electrical and thermal energy. As shown in Figure 4, increasing the WWR from 20% to 100% results in a significant rise in summer electricity production for the case buildings: from 205.56 kWh to 1018.58 kWh in Beijing, from 156.79 kWh to 777.32 kWh in Hefei, and from 129.34 kWh to 386.59 kWh in Guangzhou.

Under a given WWR, the electricity production of the buildings in Beijing surpasses that of the buildings in Hefei and Guangzhou. This discrepancy is attributed to the greater solar irradiation on the south facade of the building due to Beijing's higher latitude. In the northern hemisphere, higher latitudes result in a lower solar altitude angle, thereby increasing the intensity of solar irradiation received by the south-facing facade of a building.

3.2 Impact of WWR on heat recovery

An increase in the WWR extends the flow distance for the supply air passing through the STPV-W. Besides, a larger STPV-W areagenerates more excess heat from the PV modules. The lengthening of the flow channel further enhances the air heating performance, increasing the outlet air temperature after preheating by the PV window. This enhancement boosts the heat recovery capability of the channel air from the PV window. For example, in Beijing, the energy recovered by the supply air increases significantly from 539.64 kWh to 1116.58 kWh as the WWR increases from 20% to 60%. When the WWR is further increased to 100%, the recoveredenergy shows a slight rise to 1127.72 kWh.

3.3 Impact of WWR on air-conditioning energy consumption

The dew-point air introduced into the channel, with its relatively low temperature, exerts a significant cooling effect on the STPV-W,maintaining the interior side glazing temperature below 26°C for most operating hours. As the WWR increases from 20% to 60%, the STPV-W area coupled with the supply air reheating process expands correspondingly. This expansion increases the cool glazing's surface area, enhancing its ability to manage indoor heat load through radiative and convective heat exchanges with the indoor environment. Consequently, the cooling energy usage of the air-conditioning system decreases, as demonstrated by a reduction from 3019.56 kWh to 2969.55 kWh in the case study conducted in Beijing. However, as the WWR increases from 60% to 100%, the cooling capacity of the introduced supply air becomes constrained. Despite extending the flow path to prolong the residence time of the supply air within the channel, the temperature of the indoor-side glass does not decrease significantly. As a result, the energy consumption of the air-conditioning system experiences a slight increase, reaching 2992.20 kWh.

In Hefei and Guangzhou, the variation in the energy use for air conditioning aligns with the trend observed in Beijing, initially decreasing and then slightly increasing. Overall, as shown in Figure 5, the air-conditioning energy consumption in Hefei decreases from 3083.67 kWh to 3040.63 kWh, while in Guangzhou, it drops from 3381.20 kWh to 3320.89 kWh. For a specific WWR, the highest energy consumption for air conditioning is observed in Guangzhou, followed by Hefei, and then Beijing. This pattern is attributed to the latitudes of these cities, with Guangzhou being the southernmost, followed by Hefei, and Beijing being the northernmost. Higher latitudes generally experience higher outdoor ambient temperatures in summer, which enhances both convective and radiative heat transfer between indoor and outdoor environments. As a result, the heat gain through the building envelope increases, leading to greater cooling energy consumption.

3.4 Impact of WWR on fan energy and lighting energy

Fan power is closely tied to the supply airflow rate of the air-conditioning system, which correlates with the variation in room coolingload. In Beijing, for instance, as the WWR increases, fan energy requirement initially decreases from 1052.29 kWh to 1029.41 kWh, before rising slightly to 1036.77 kWh. Additionally, enlarging the window area allows more daylight penetration into the interior thus reducing artificial lighting demands from 1664.02 kWh to 372.90 kWh.

3.5 Impact of WWR on overall energy performance

As illustrated in Figure 5, an increase in WWR from 20% to 100% results in a substantial decrease in the total summer NEC of the case buildings. In Beijing, this consumption drops from 4990.68 kWh to 2255.58 kWh, in Hefei from 5169.58 kWh to 2554.12 kWh, and in Guangzhou from 5602.85 kWh to 3253.11 kWh. These reductions correspond to 54.80%, 50.59%, and 41.94%, respectively. This data indicates that increasing the WWR enhances the energy efficiency of buildings utilizing this combined STPV-W system, with more pronounced effects observed in higher latitude cities in China.

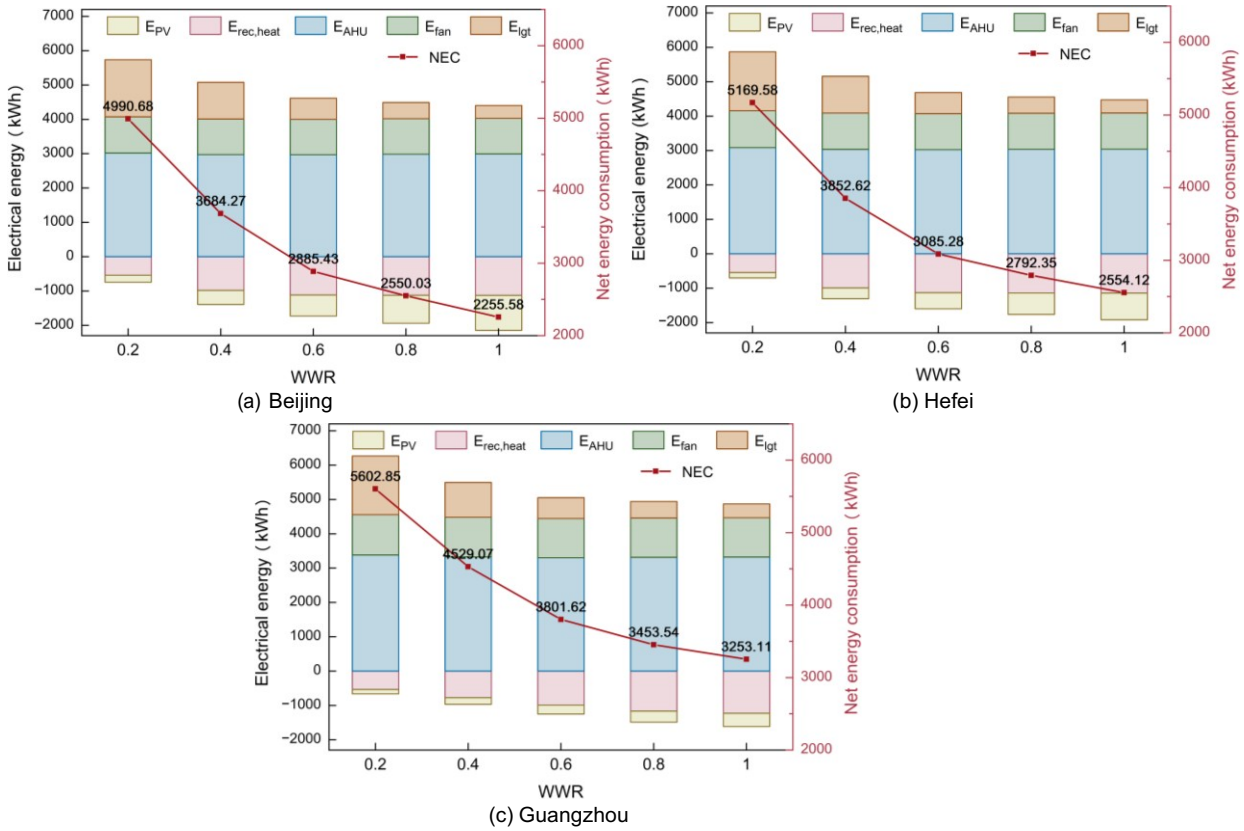

(a) Beijing (b) Hefei

(c) Guangzhou

Figure 4: Energy benefits and consumption, and NEC for different WWR

4. CONCLUSION

This study evaluated the impact of the WWR on the performance of STPV-W integrated with an air-conditioning system. An optical- thermal-electrical model was developed using Matlab, and artificial lighting energy demand was simulated with DesignBuilder.

The results indicate that increasing the WWR significantly enhances building performance, particularly in higher latitude regions of China, such as Beijing. A WWR of 60% or higher is recommended. As the WWR increases from 20% to 100%, electricity production and waste heat recovery from PV windows rise. The air-conditioning load and fan energy initially decrease before slightly increasing, while lighting energy consumption reduces due to increased natural light availability. Overall, expanding the STPV-W area reduces the NEC of the buildings in summer in Beijing, Hefei, and Guangzhou by 54.80%, 50.59%, and 41.94%, respectively. In summary, increasing the WWR is an effective approach to optimizing the architectural design of buildings that integrate STPV-W and advanced air handling processes, thereby enhancing energy-saving potential.

5. REFERENCES

QIU, C. & YANG, H. 2022. Dynamic coupling of a heat transfer model and whole building simulation for a novel cadmium telluride- based vacuum photovoltaic glazing. Energy, 250.

SKOPLAKI, E. & PALYVOS, J. A. 2009. On the temperature dependence of photovoltaic module electrical performance: A review of efficiency/power correlations. Solar Energy, 83**,** 614-624.

TAN, Y., PENG, J., LUO, Y., LI, H., WANG, M., ZHANG, F., JI, J. & SONG, A. 2023. Daylight-electrical-thermal coupling model forreal-time zero-energy potential analysis of vacuum-photovoltaic glazing. Renewable Energy, 205**,** 1040-1056.

TANG, Y., JI, J., WANG, C., XIE, H. & KE, W. 2022. Combining photovoltaic double-glazing curtain wall cooling and supply airreheating of an air-conditioning system: Energy-saving potential investigation. Energy Conversion and Management, 269.

WANG, C., UDDIN, M. M., JI, J., YU, B. & WANG, J. 2021. The performance analysis of a double-skin ventilated window integratedwith CdTe cells in typical climate regions. Energy and Buildings, 241**,** 110922.

WANG, M., PENG, J., LI, N., LU, L., MA, T. & YANG, H. 2016. Assessment of energy performance of semi-transparent PV insulatingglass units using a validated simulation model. Energy, 112**,** 538-548.

YADAV, S. & HACHEM-VERMETTE, C. 2024. Performance evaluation of semitransparent PV window systems employing periodicthermal model. Applied Energy, 353.

YOUNT, F. 2017. ASHRAE Handbook committee, ASHRAE Handbook–Fundamentals. ASHRAE.

ZHANG, C., JI, J., WANG, C. & KE, W. 2024. Annual analysis and comparison of the comprehensive performance of a CdTe PVventilated window integrated with vacuum glazing in different climate regions. Renewable Energy, 223.